Simple method for absolute calibration of geophones, seismometers, and other inertial vibration sensors

Cite as: Rev. Sci. Instrum. **76**, 034501 (2005); https://doi.org/10.1063/1.1867432
Submitted: 27 April 2004 . Accepted: 28 December 2004 . Published Online: 22 February 2005

Frank van Kann, and John Winterflood

Simple method for absolute calibration of geophones, seismometers, and other inertial vibration sensors

Frank van Kann and John Winterflood
School of Physics, The University of Western Australia, Nedlands, WA, 6009, Australia

(Received 27 April 2004; accepted 28 December 2004; published online 22 February 2005)

A simple but powerful method is presented for calibrating geophones, seismometers, and other inertial vibration sensors, including passive accelerometers. The method requires no cumbersome or expensive fixtures such as shaker platforms and can be performed using a standard instrument commonly available in the field. An absolute calibration is obtained using the reciprocity property of the device, based on the standard mathematical model for such inertial sensors. It requires only simple electrical measurement of the impedance of the sensor as a function of frequency to determine the parameters of the model and hence the sensitivity function. The method is particularly convenient if one of these parameters, namely the suspended mass is known. In this case, no additional mechanical apparatus is required and only a single set of impedance measurements yields the desired calibration function. Moreover, this measurement can be made with the device *in situ*. However, the novel and most powerful aspect of the method is its ability to accurately determine the effective suspended mass. For this, the impedance measurement is made with the device hanging from a simple spring or flexible cord (depending on the orientation of its sensitive axis). To complete the calibration, the device is weighed to determine its total mass. All the required calibration parameters, including the suspended mass, are then determined from a least-squares fit to the impedance as a function of frequency. A demonstration using both a 4.5 Hz geophone and a 1 Hz seismometer shows that the method can yield accurate absolute calibrations with an error of 0.1% or better, assuming no *a priori* knowledge of any parameters. © *2005 American Institute of Physics.* [DOI: 10.1063/1.1867432]

I. INTRODUCTION

Geophones are sensitive instruments for measuring vibrations at low audio frequencies. Their low cost, ruggedness, reliability, and ease of use makes them useful in many applications, apart from the standard one of seismic surveying. An absolute calibration is not always required and calibration data are not readily available for some commercial devices. For mass produced devices, only typical data are given and these might be of insufficient accuracy. Even if calibration data are available, the calibration is likely to change with time due mainly to aging of either or both the permanent magnet or suspension mechanism. Similar arguments apply to seismometers and other inertial vibration sensors.

Therefore, for those applications where calibration is required, shaker platforms have often been used. Apart from being expensive and cumbersome, these are not commonly available and rely on the availability of a reference sensor whose calibration is known to sufficient accuracy. Laser interferometers have been used[1] for this but make the apparatus more complex. Several authors have suggested alternate calibration methods which exploit the reciprocity of the transducer. These are based on either transient methods[2–6] or spot measurements of the phase of the impedance.[2,7–12] Both techniques are described in some detail by Asten[2] but both are limited by the accuracy with which the suspended mass is known, which cannot be determined by these procedures. The impedance method described by Lin Jin[6] can determine the suspended mass but is restricted to specially designed devices which provide access to the internal mechanism and would not be practical in the field.

This paper presents a new method of obtaining an absolute calibration for any geophone or inertial vibration sensor, which exploits the reciprocity in a novel way to obtain all of the parameters required to characterize the device, including the effective suspended mass if required. There are two variants of the method, depending on whether or not the suspended mass of the sensor is known and in both cases the parameters are derived from a measurement of the impedance as a function of frequency.

This method requires only elementary equipment readily available in the field. The simpler variant may be used when the suspended mass is known to sufficient accuracy. In this case, it is similar to existing techniques such as the phase ellipse method[8] except that this new method gives all the other parameters, including the inductance and resistance of the coil from the single measurement. This is because the method records both the amplitude and phase over a broad spectrum of frequencies (rather than finding the 2 or 3 special frequencies as in the example of the phase ellipse method). The impedance can be measured with the device *in situ* and all of the parameters are obtained with corresponding accuracy by this single measurement.

The extended variant must be used when the suspended mass is not known. However, even in cases where the sus-

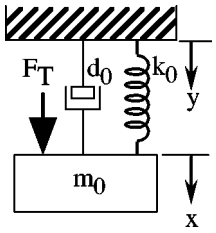

FIG. 1. Mechanical model of the vibration sensor.

pended mass is quoted by the manufacturer, it is useful to use the extended method to verify the mass, since the specified value might be of insufficient accuracy or, as found in at least one case, incorrect.

The calibration method is based on the standard mechanical model[13] of an inertial vibration sensor, which is described (with particular reference to geophones) in Secs. II and III. Section IV outlines how the model gives the sensitivity of the sensor as a function of frequency. This is followed in Sec. V by a description of the equivalent electrical model of the device, which is characterized entirely by its impedance.

The calibration procedure for the two cases, depending on whether or not the mass of the moving part is known, is developed in the subsequent four sections, with example data from the calibration procedure for both a typical geophone (a model L15) and a typical seismometer (a model L4) manufactured by Mark Products Inc.[14]

Finally, an experimental verification of the calibration is described in Sec. X.

II. SENSOR MODEL

An inertial vibration sensor consists of a damped resonant mass constrained in a housing to move in one dimension parallel to the sensitive axis. A mechanical model for the geophone with its housing fixed to the Earth's surface (or to any object whose vibrations are to be measured) is shown in Fig. 1.

In this example, the sensitive axis is vertical but horizontal configurations are equally common.

The analysis is most conveniently performed using the complex Laplace transform and a glossary of symbols used in the model is given in Table I.

The notation adopted is such that signals in the time domain are represented in lower case, and for each one the corresponding signal in the frequency domain is represented by the corresponding upper case character.

III. ANALYSIS OF THE GEOPHONE MODEL

In the configuration of Fig. 1, the device is clamped to the Earth's surface and thus the housing motion $\dot{y}$ corresponds to the seismic motion of the Earth's surface.

A transducer senses the relative motion between the mass and housing to produce an electrical signal V_S, which is modeled as the Thevenin equivalent circuit shown in Fig. 2.

All sources of noise are ignored as they are not required for the purpose of obtaining the sensitivity of the device.

In Fig. 2, Z_{22} is the output impedance of the transducer and Z_L is the load impedance. The latter is usually in the form of a resistor connected in parallel with the output to provide the desired damping characteristic but may also include stray capacitance at the input of the amplifier and in the connecting cable. The amplifier, with frequency response function $A(f)$, provides the necessary gain and filtering for data acquisition.

TABLE I. Glossary of symbols.

Time	frequency	description
y	Y	vertical component of the housing position
$\dot{y}$	sY	vertical component of the housing velocity
$\ddot{y}$	s^2Y	vertical component of the housing acceleration
x	X	vertical component of the sensor proof mass position
m_0		mass of suspended sensor mass
k_0		mechanical spring constant of sensor suspension
d_0		viscous damping coefficient of sensor suspension
f_0		resonance frequency of sensor (unloaded)
Q_0		quality factor of sensor resonance
m_1		mass of housing and associated fixtures
m_e		effective mass of the housing suspension (spring or cord)
k_1		effective spring constant of housing suspension, including umbilical
d_1		viscous damping coefficient of housing suspension
f_T	F_T	force from transducer on suspended mass of sensor
v_S	V_S	Thevenin equivalent voltage source of transducer
v_T	V_T	voltage of loaded transducer
i_T	I_T	current flowing in the transducer
L_T	Z_{L_T}	inductance of the transducer coil
R_T		resistance of the transducer coil
f		frequency (Hz)
	s	variable in the frequency domain, $s=j2\pi f$; $j=\sqrt{-1}$

The signal from the geophone is given by the standard equation[13,15] for a passive transducer

$$\begin{pmatrix} F_T(f) \\ V_T(f) \end{pmatrix} = \begin{pmatrix} Z_{11} & Z_{12} \\ Z_{21} & Z_{22} \end{pmatrix} \begin{pmatrix} s(X(f) - Y(f)) \\ I_T(f) \end{pmatrix}, \tag{1}$$

where Z_{ij} is the transimpedance matrix of the transducer and the other terms are defined in the glossary. For a passive transducer, energy conservation requires that $Z_{12} = \pm Z_{21}$ (reciprocity),[13] where the sign depends on the type of transducer.[16]

The open circuit or unloaded condition corresponds to $i_L = 0$ and in this case the output is

$$V_T(f) = V_S(f) = Z_{21}(f)s(X(f) - Y(f)), \tag{2}$$

where the factor $Z_{21}(f)$ depends on the nature of the transducer and in some cases is a function of the frequency. Most geophones use an inductive transducer, for which $Z_{12} = -Z_{21}$

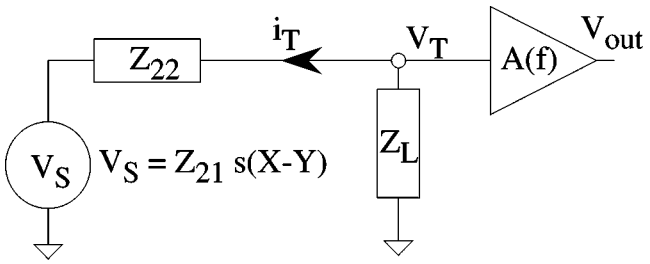

FIG. 2. Thevenin equivalent circuit of the signal source for the vibration sensor.

is a constant, namely $Z_{12}=B\ell$, where B is the effective magnetic field of the permanent magnet and ℓ is the effective length of wire in this field.

The output impedance is Z_{22}. For an inductive transducer this is the impedance of the coil which produces the signal and at sufficiently low frequency, this is simply the resistance of the coil in series with its inductance. At higher frequencies, the interwinding capacitance becomes important, as does the hysteretic loss in the core of the coil. The former produces a low Q factor resonance (see Fig. 7 below), while the latter is nonlinear and not easily modeled in terms of simple passive components.

Thus, for sufficiently low frequencies,

$$Z_{22} \approx R_T + sL_T. \tag{3}$$

In the presence of a finite load impedance Z_L the loaded output signal $V_T(f)$ is a measure of the velocity $sY(f)$ of the geophone housing and is given by

$$V_T(f) = K(f)sY(f), \tag{4}$$

where $K(f)$ is the sensitivity function of the device.

IV. SENSITIVITY OF THE VIBRATION SENSOR

The sensitivity function $K(f)$ can be written as the product of its constituent terms in the form

$$K(f) = G(f)Z_{12}(f)H(f), \tag{5}$$

where $G(f)$ is the attenuation factor due to the loading of the output impedance, and $H(f)$ is the transfer function of the mechanical resonator, when coupled to the loaded transducer. These are, respectively,

$$G(f) = \frac{Z_L}{Z_L + Z_{22}} \tag{6}$$

and

$$H(f) = \frac{\left(\frac{f_0'}{f_0}\right)^2\left(\frac{f}{f_0'}\right)^2}{1-\left(\frac{f}{f_0'}\right)^2 + \frac{j}{Q_0'}\left(\frac{f}{f_0'}\right)}, \tag{7}$$

where f_0' is the loaded resonance frequency and Q_0' the loaded quality factor of the resonance. These are given in terms of the intrinsic, unloaded mechanical resonance parameters f_0 and Q_0 by the approximations

$$f_0' \approx f_0\left(1 + \frac{Z_{12}^2 L_T}{m_0(R_T+R_L)^2}\right) \tag{8}$$

and

$$Q_0' \approx \frac{Q_0}{1+\frac{Z_{12}^2}{d_0(R_T+R_L)}}. \tag{9}$$

These results are easily derived from the impedance formalism described in Sec. VI.

Equation (9) describes the additional damping produced by the load resistance and a more familiar form is

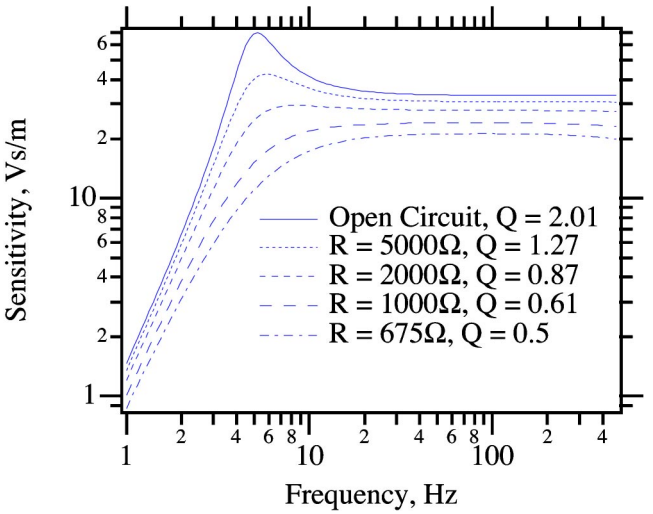

FIG. 3. (Color online) Sensitivity curves for the L15 geophone.

$$d_0' \approx d_0 + \frac{Z_{12}^2}{(R_T+R_L)}, \tag{10}$$

which is often quoted (usually normalized to critical damping) in the manufacturer's specification for a geophone. The corresponding change in resonance frequency described by Eq. (8) is much smaller and is usually ignored.

The unloaded case, $Z_L=\infty$, is approximated by $|Z_L| \gg |Z_{22}|$ and in this case,

$$G(f) \approx 1, \quad f_0' \approx f_0 = \frac{1}{2\pi}\sqrt{\frac{k_0}{m_0}} \tag{11}$$

and

$$Q_0' \approx Q_0 = \frac{2\pi f_0 m_0}{d_0}. \tag{12}$$

The function $K(f)$ is often plotted by the geophone manufacturer for several values of load resistance ($Z_L=R_L$). This provides additional damping and the value of R_L which gives the flattest sensitivity curve is often used. In many cases, a resistor of this value is installed by the manufacturer and must be either removed or taken into account during the calibration.

An example of the sensitivity function for the L15 geophone is shown in Fig. 3.

At frequencies sufficiently above the resonance peak, the curves are approximately flat and this defines the useful frequency band of the device. However, the sensitivity drops slightly above a few hundred Hz, where the increase in output impedance, due to the series inductance acting as a voltage divider with the load impedance, becomes significant. The curves in Fig. 3 are consistent with those published by the manufacturer.

Note that the form of the sensitivity function $K(f)$ in the useful frequency band does not depend individually on either m_0 or k_0 but only on the ratio $k_0/m_0=(2\pi f_0)^2$. Indeed, the dependence on f_0 is rather weak; although f_0 and Q_0 determine the useful frequency band, the sensitivity within this band is almost independent of either. Therefore, the absolute

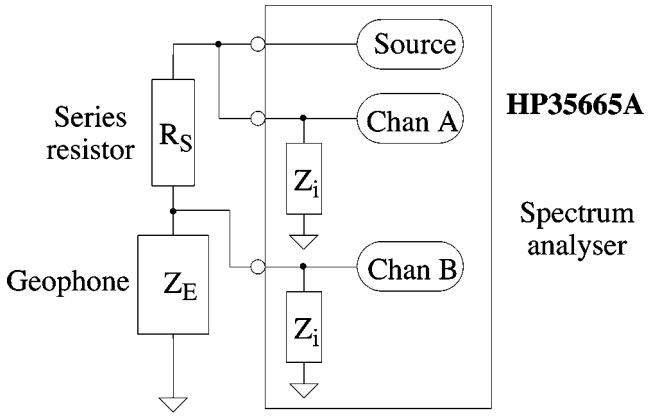

FIG. 4. Block diagram of the calibration procedure.

calibration of the geophone for the unloaded case depends mainly on the parameter Z_{12}, with some weak dependence on f_0 and Q_0.

However, a common configuration is to operate the geophone loaded with the appropriate resistance to give the desired damping and in this case the parameters R_T and L_T (in addition of course to R_L) are also required. These could be obtained from direct electrical measurement of the impedance at the output terminals of the device. However, such a measurement is not entirely straight forward since the electrical properties are strongly dependent on the mechanical behavior, as outlined in the next section.

V. EQUIVALENT IMPEDANCE OF THE SENSOR

The observed electrical impedance between the output terminals of the geophone, seismometer or other passive inertial vibration sensor is given by

$$Z_E = Z_{22} - \frac{Z_{12}Z_{21}}{Z_m}, \tag{13}$$

where Z_m is the mechanical impedance of the device, defined by analogy with Ohm's law as

$$Z_m = \frac{F_T}{sX} = \frac{k_0}{s}\left(1 + \frac{s^2 m_0}{k_0} + \frac{s d_0}{k_0}\right). \tag{14}$$

For the inductive transducer, this gives

$$Z_E = R_T + j2\pi f L_T + \frac{j2\pi f Z_{12}^2}{m_0(2\pi f_0)^2\left(1 - \left(\frac{f}{f_0}\right)^2 + \frac{j}{Q_0}\left(\frac{f}{f_0}\right)\right)}. \tag{15}$$

The parameters of this function can be obtained experimentally by a least-squares fit to a set of measurements of the impedance made at several frequencies in a suitable frequency band.

It is evident that the parameters Z_{12} and m_0 are not separable and only the ratio Z_{12}^2/m_0 can be obtained, whereas the remaining parameters f_0, Q_0, R_T, and L_T required for the calibration can be found separately.

In the case where m_0 is known independently, the entire calibration is given by this procedure.

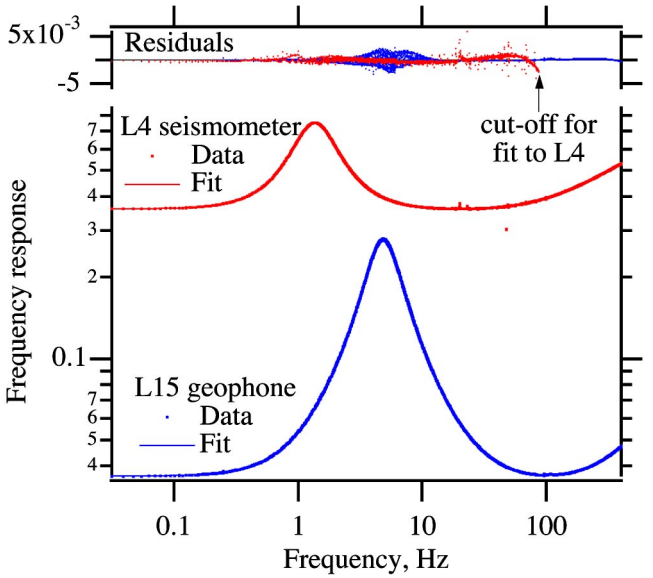

FIG. 5. (Color online) Frequency response for the L15 geophone and L4 seismometer.

VI. CALIBRATION PARAMETERS OBTAINED FROM THE MEASURED IMPEDANCE

The block diagram of the arrangement used for the impedance measurement is shown in Fig. 4. Apart from the geophone, only a single resistor R_S is required. The impedance Z_E is obtained from the ratio of the voltage divider formed by R_S and Z_E.

In Fig. 4 a FFT spectrum analyzer (Model HP35665A from Agilent, formerly Hewlett Packard) is used to measure this ratio as a frequency response or transfer function.

The signal source is programmed to produce a periodic chirp, which has a "white" spectrum, but random noise with a similar spectrum would also be suitable. If a spectrum analyzer is not available, a data logger with at least two input channels and one output can be used.

In either case, the input impedance Z_i of the instrument must be taken into account and the measured frequency response corresponds to the complex ratio

$$\rho(f) = \frac{Z_E'}{Z_E' + Z_S'}, \tag{16}$$

where Z_E' represents the impedance of Z_E in parallel with the input impedance Z_i of the analyzer and similarly for Z_S', with

$$Z_S' = \frac{R_S Z_i}{R_S + Z_i} \text{ and } Z_E' = \frac{Z_E Z_i}{Z_E + Z_i}. \tag{17}$$

An example of applying the calibration procedure for the L15 geophone is shown in Fig. 5.

This geophone provides a useful test because reasonably comprehensive calibration data are quoted by the manufacturer. Some of these, including Z_{21}, f_0, Q_0, and L_T are susceptible to drifts because of aging and fatigue. Others such as m_0 and R_T are likely to be more stable. In particular, the suspended mass is quoted with reasonable precision, so that the full calibration can be obtained from the single impedance measurement.

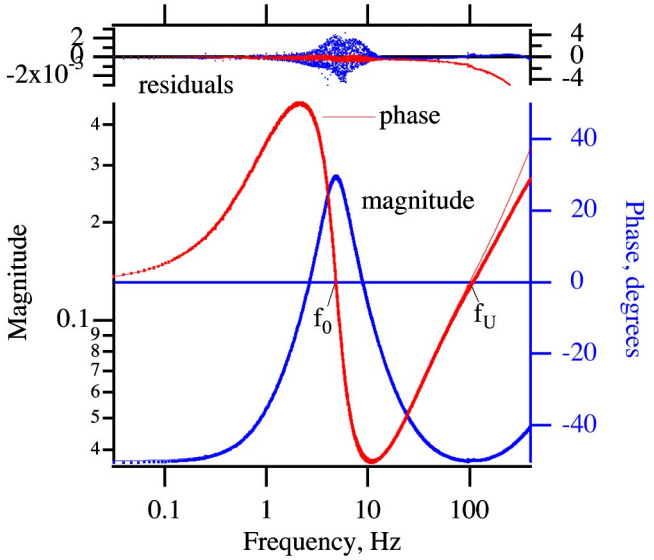

FIG. 6. (Color online) Magnitude and phase of the impedance for the L15 geophone.

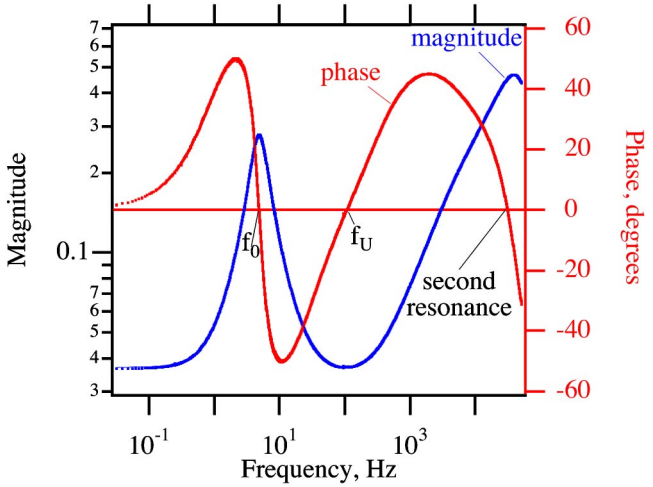

FIG. 7. (Color online) Second resonance of the L15 geophone.

For comparison, the L4 seismometer from the same manufacturer was also calibrated in this way. The magnitude of $\rho(f)$ for both is plotted as the solid dots in Fig. 5.

As indicated on the graph, the lower data set corresponds to the L15 and the upper data is for the L4. The resonance peak is clearly seen for both devices, with the L4 having a much lower resonance frequency than the L15.

For each data set, the best fit function is plotted as a continuous smooth curve, which for both devices is close to the data, indicating excellent agreement with the model. Some random scatter is evident from the residuals, which are plotted on an expanded scale above the data.

Also evident from the residual plot is the systematic error at the upper end of the frequency interval, particularly for the L4 with its large inductance. The departure from the model of the L4 is so large that the data above 100 Hz (depicted in Fig. 5 by the arrow labeled "cut-off for L4") are not included in the fit. This indicates that, as outlined in Sec. IV, the output impedance is not well modeled as a simple inductance in series with a resistance. This is attributed to the magnetic properties of the material of the core (rather than the interwinding capacitance which becomes important at higher frequency) but further investigation would be needed to explore this.

Fortunately, the frequency at which this systematic error becomes significant, compared to the random errors, is well above the resonance and does not affect the determination of the parameters associated with the resonance. The calibration is therefore not significantly affected.

The calibration procedure described above has some similarities with the commonly used "phase ellipse" method. Although only the magnitude of the impedance is used for curve fitting, the phase is also measured and that for the L15 is shown in Fig. 6, together with the magnitude data from Fig. 5. The measured phase data are plotted as solid dots and the model function for the phase, calculated using the parameters obtained from the fit to the magnitude, is plotted as a smooth curve. The residuals for both amplitude and phase are also shown. Again, the systematic error at high frequency is evident.

Figure 6 clearly shows that the resonance frequency corresponds to the point at which the phase curve crosses zero, labeled as f_0. The phase also crosses zero at a second frequency, labeled as f_U. This frequency is often referred to as the upper resonance frequency after Asten.[2] However, as Fig. 6 shows, it is not appropriate to call it a resonance, although it would become a resonant dip if the coil resistance were sufficiently reduced. This is not the case in either the L4 or L15 and probably not in any practical geophone operated at room temperature without feedback.

There is often a second resonance at much higher frequency, which is produced by the combination of the inductance of the sensor coil combined with capacitance. This arises from interwinding capacitance of the coil and capacitance of the connecting cables. The observed second resonance for the L15 is shown in Fig. 7.

The parameter values obtained using the spectrum fitting method are generally in good agreement with the quoted values, as shown in Table II.

TABLE II. Parameters for the L15 geophone and L4 seismometer.

	L15 geophone	
Parameter	Best fit	Quoted
m_0(g)	23 (fixed)	23.00±0.01
f_0(Hz)	4.847±0.001	4.5±0.5
Q_0	2.011±0.001	1.8±0.2
Z_{12}(V m^{-1} s)	33.8±0.003	33.1±3
$R_T(\Omega)$	376.6±0.2	375±38
L_T(H)	0.139±0.003	
	L4 seismometer	
Parameter	Best fit	Quoted
m_0(g)	982.6 (fixed)	982.6±0.1
f_0(Hz)	1.363±0.001	1.0±0.05
Q_0	2.933±0.003	2.5±0.2
Z_{12}(V m^{-1} s)	268.8±0.06	276±1
$R_T(\Omega)$	5579±1	5500±50
L_T(H)	4.90±0.01	6.0±0.6

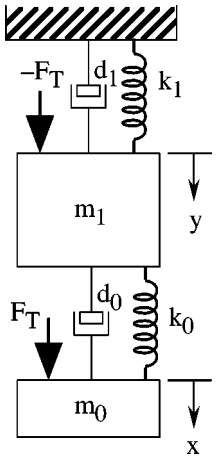

FIG. 8. Mechanical model of the suspended vibration sensor.

Apart from the frequency no uncertainties are given for the quoted parameters and these are inferred from the number of digits specified. However, this is likely to be somewhat optimistic for these mass-produced devices.

An analysis of the covariance[17] shows that the parameters are statistically independent, apart from a slight correlation between Z_{12} and Q_0. However, this is not significant and the fitted parameter uncertainties listed in Table II correspond to the 95% confidence interval for the fit.

In both cases, the frequency is somewhat higher than the quoted value and for the L4 is outside the specified range. The L4 used in the experiment was manufactured in 1979 and the frequency may have been increased by 30% because of shock damage to the spring or magnet during its life.

VII. CALIBRATION WHEN THE SUSPENDED MASS IS NOT KNOWN

To obtain the calibration parameters when the suspended mass m_0 is not known, the extended variant of the method is required, using a configuration which allows Z_{12} and m_0 to be separated. This can be obtained simply by suspending the geophone from a spring, to introduce a second normal mode. This measurement replaces and extends the fixed sensor method described in the previous section (Sec. VI).

The mechanical configuration for the suspended geophone is shown in Fig. 8 and shows the entire geophone suspended from spring k_1 (with associated damping d_1). It is modeled as a one-dimensional system, with two degrees of freedom. In this example the axis is vertical but horizontal configurations are similar.

For horizontal sensors, instead of using a spring, the device would be hung from flexible cord to form a pendulum in which the sensitive axis of the sensor is kept horizontal.

The total mass of the hanging system is $M=m_1+m_0+m_e$, where m_0 is the suspended mass of the sensor, m_1 the mass of the remaining parts of the device, including the housing and other fixtures and m_e is the effective mass of the spring (or pendulum cord) from which the device is hung. The mass m_1+m_0 can be obtained simply by weighing the device with a balance or scale of sufficient accuracy. However, the effective mass of the spring must also be taken into account and for a linear spring of total mass m_S, the effective mass (that part participating in the motion) is $m_e=m_S/3$.

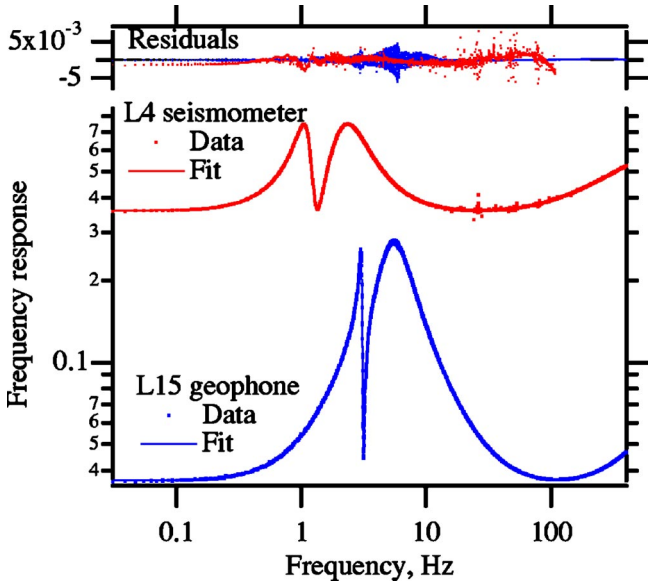

FIG. 9. (Color online) Calibration data for the suspended L15 geophone and L4 seismometer.

The stiffness of the spring or the length of the pendulum should be chosen so that the two normal-mode frequencies are similar; that is they should be separated by less than the bandwidth of the modes.

VIII. ANALYSIS OF THE TWO-MODE SYSTEM

The mechanical impedance of the two-mode system shown in Fig. 8 is

$$Z_m = \frac{F_T}{s(X-Y)} = \frac{\left(m_1 s + d_1 + \frac{k_1}{s}\right)\left(m_0 s + d_0 + \frac{k_0}{s}\right) + m_0 s\left(d_0 + \frac{k_0}{s}\right)}{m_1 s + m_0 s + d_1 + \frac{k_1}{s}}. \tag{18}$$

The equivalent electrical impedance is as given before by Eq. (11),

$$Z_E = Z_{22} - \frac{Z_{12}Z_{21}}{Z_m},$$

but using the modified form of Z_m.

IX. CALIBRATION FOR THE HANGING SENSOR

Again (as in the case where the suspended mass is known), the spectrum analyzer is used to obtain the impedance from a measurement of the ratio $\rho(f)$. The data for the L15 and the L4 in the hanging configuration are shown in Fig. 9.

These devices are designed for sensing vertical motion and were hung from a simple coil spring using wire and adhesive tape to attach the device to the spring. The other end of the spring was attached to a convenient hook on the

TABLE III. Parameters for the L15 geophone and the L4 seismometer.

Parameter	L15 geophone Best fit	Quoted
m_0(g)	22.99±0.03	23.00±0.01
f_0(Hz)	4.881±0.003	4.5±0.5
Q_0	1.998±0.002	1.8±0.2
Z_{12}(V m^{-1} s)	34.528±0.008	33.1±3
R_T(Ω)	376.1±0.3	375±38
L_T(H)	0.1132±0.0004	
M(g)	144.6 (fixed)	
f_1(Hz)	2.552±0.002	
Q_1	1200±10	
Parameter	**L4 seismometer Best fit**	**Quoted**
m_0(g)	965.2±0.4	982.6±0.1
f_0(Hz)	1.364±0.001	1.0±0.05
Q_0	2.95±0.002	2.5±0.2
Z_{12}(V m^{-1} s)	266.3±0.05	276±1
R_T(Ω)	5596±1	5500±50
L_T(H)	4.69±0.01	6.0±0.6
M(g)	2173 (fixed)	
f_1(Hz)	1.812±0.001	
Q_1	98±4	

ceiling. To avoid an unwanted pendulum mode near one of the desired normal modes, the spring was extended by a length of wire to move the pendulum frequency out of the band of interest.

The format of Fig. 9 is similar to Fig. 5. The data (plotted as the solid dots) clearly show the two normal modes of each device. The original internal mode of each sensor is moved to a slightly higher frequency due to the reduced mass effect and retains its relatively low quality factor. The second mode has a different frequency and by choice is within the bandwidth of the first.

The best-fit function for each data set is plotted as the smooth curve, which is in good agreement with the data, apart from some scatter near the resonance peaks. This is evident in the graph of the residuals, plotted above the data.

This also indicates the presence of some spectral lines in the data for the L4. These are resonances internal to the device, the lowest being at 22.5 Hz. This is outside the range of the sensitivity curves quoted by the manufacturer, which are truncated at 20 Hz.

The systematic error due to the nonlinear properties of the inductance is again discernible.

The best-fit parameters for both devices are listed in Table III, together with the quoted values for comparison. The last three parameters do not have quoted values as they are peculiar to the calibration procedure.

For both sensors f_0 and f_1 are sufficiently close, and it is unimportant that for the L15 $f_1 < f_0$ whereas the converse is true for the L4, with $f_1 > f_0$.

The parameter values for the L15 are in excellent agreement with those obtained previously with the sensor fixed. In particular, the mass m_0 and sensitivity coefficient Z_{12} obtained by both methods is consistent and within the tolerance

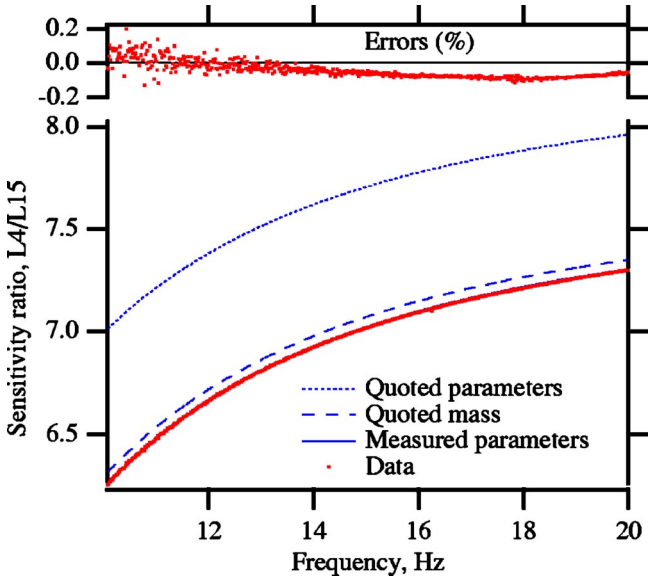

FIG. 10. (Color online) Measured sensitivity ratio of the L4 and L15.

band of the quoted value. The mass obtained from the fit is consistent with the quoted value to the number of digits specified.

For the L4 the agreement between the parameters obtained from the calibration and the quoted values is not so good. In particular, the mass is nearly 2% less than the quoted value, even though the latter is given to 4 significant digits, with an implied accuracy of 0.1% or better. Moreover, the sensitivity is more than 3% below the quoted value. Since the fit to the model is good, it is possible that the quoted parameters are incorrect. This possibility is tested in the next section.

X. VERIFICATION OF THE CALIBRATION

A definitive test of the calibration procedure is to directly compare the sensitivities of the two devices over a useful overlapping range of frequencies for the two.

For this, the two devices were bonded together and suspended from the cone of a heavy duty loudspeaker. The suspension of this is sufficiently stiff to support the weight of both the L4 and L15 without exceeding its available travel range. The speaker was driven by a chirp signal with a flat spectrum from 10 to 20 Hz.

To avoid spurious electromagnetic coupling between the geophones, they were separated by a rigid plastic spacer. For the same reason, a one metre long non-magnetic rod was used to separate the geophones from the speaker. As described below, the results obtained verify that spurious magnetic coupling is not a problem.

The response of both sensors was recorded using the spectrum analyzer, with the observed frequency response being a measure of the ratio of the sensitivity functions for the two devices,

$$|\rho(f)| = \frac{|K_{\mathrm{L4}}(f)|}{|K_{\mathrm{L15}}(f)|}, \tag{19}$$

where $|\rho(f)|$ is the magnitude of the measured frequency response, $|K_{\mathrm{L4}}(f)|$ is the magnitude of the sensitivity function

for the L4 and $|K_{L15}(f)|$ that of the L15. In both cases, the load impedance is taken to be the input impedance of the spectrum analyzer.

This ratio is plotted in lower part of Fig. 10, where the solid dots represent the measured ratio. The three smooth curves show the prediction calculated from three different sets of parameter values.

The first set consists of the values quoted by the manufacturer. These are listed in Table II (and again in Table III) in the columns titled "Quoted." This gives the dotted curve, which is obviously a very poor model for the data. Most of the discrepancy is due to the sensitivity factor Z_{12}, which for the L15 is about 3% higher than specified and for the L4 about 3% lower.

The second set consists of the quoted mass together with the corresponding calibration parameters measured with the sensors fixed. These are the values which would be obtained using any of the existing calibration methods which require the suspended mass to be known. They are listed in Table II in the columns titled "Best fit." This gives the dashed curve, which although it is much closer to the data is still a poor model, falling many times beyond standard deviation of the noise.

Finally, the third set consists of the parameters obtained by the new calibration procedure for both devices, listed in Table III in the columns titled "Best fit." This gives the solid curve and is clearly an excellent match to the data, with a root-mean-square deviation of 0.07% over the interval from 10 Hz to 20 Hz. The deviations, labeled "Errors (%)" are plotted in the upper part of Fig. 10.

It is emphasized that there are no free parameters in any of the smooth curves; they are calculated from the previously obtained calibration parameters. The close agreement between the data and the solid curve is consistent with the hypothesis that the quoted mass for the L4 is incorrect and that the calibration procedure gives the correct parameters.

XI. DISCUSSION

The calibration method described in Sec. VI is similar to existing methods, which require the suspended mass of the sensor to be known, but is more convenient than many of these existing methods since it requires only a single standard electronic instrument. Like many of the existing methods, the calibration can be performed with the sensor *in situ*.

The new method presented in this paper is able to determine the effective suspended mass of the sensor, which is not possible with the existing methods. In this case it is not quite as convenient because the measurement cannot be performed *in situ* and ideally requires the sensor to be removed from its weatherproof deployment enclosure. Fortunately, the mass is likely to remain constant and need only be determined once for a particular device, after which the remaining parameters can be determined whenever desired with the device *in situ*. Also, for mass produced devices, it may be sufficient to determine the suspended mass for only a single unit or a small sample of a particular model.

The new method has been successfully tested with two vertical axis sensors, the L15 and L4, which cover a large range of size, resonance frequency and sensitivity. For the L15, the obtained calibration is in good agreement with that quoted by the manufacturer. However, for the L4 the agreement is not good. The mass obtained is some 2% different from the quoted value and this error is almost two orders of magnitude larger than the uncertainty.

An independent verification has been performed, by directly comparing the calibrations of the two devices, which shows that the two calibrations agree within a root-mean-square error of only 0.07%. This suggests that the quoted parameters are incorrect and that the calibration procedure is able accurately to determine the sensor parameters, including the effective suspended mass. Assuming that the error is equally apportioned between the two calibrations, each is accurate to within approximately 0.05%.

This accuracy is obtained using only the magnitude of the impedance for curve fitting. It is possible that even better accuracy could be obtained using both amplitude and phase in a two-dimensional fitting procedure.

Note added in proof: The apparently anomalous result for the L4 has been explained. The manufacturer has taken an interest in the problem and offered to refurbish the device. It has been returned with a different value for the mass engraved on the specification plate. This is now 965.7 g, within 1.2 standard deviations of the value in Table III. It is possible that the mass might have been changed slightly during the refurbishment but unfortunately the original mass was not recorded at disassembly. The calibration procedure has been repeated for the refurbished device and both the mass and resonance frequency are within 1 standard deviation of the specified values.

[1] A. MacArthur, Geophysics **50**, 49 (1985).
[2] M. W. Asten, IEEE Trans. Geosci. Electron. **GE-15**, 208 (1977).
[3] S. P. Boughn, W. M. Fairbank, R. P. Giffard, P. F. Michelson, J. C. Price, and R. C. Taber, Rev. Sci. Instrum. **61**, 1 (1990).
[4] W. Menke, L. Shengold, Guo Hongsheng, Hu Ge, and A. Lerner-Lam, Bull. Seismol. Soc. Am. **81**, 232 (1991).
[5] T. B. Gabrielson, J. Acoust. Soc. Am. **102**, 2800 (1997).
[6] A. G. Mysh, Seismicheskie Pribory: Instrumenta'naye Sredstva Seismicheskikh Nablyudenii, **20**, 154 (1988).
[7] B. A. Palmer, Geophys. Prospect. **12**, 422 (1964).
[8] J. R. Cornett, "Transducer Testing Apparatus," U.S. Patent No. 2 648 979 (1953).
[9] H. P. Liu and L Peselnick, Geophys. Prospect. **34**, 537 (1986).
[10] H. P. Liu and E. Warrick, Geophysics **63**, 18 (1998).
[11] R. J. Donato, Bull. Seismol. Soc. Am. **61**, 641 (1971).
[12] Lin Jin, Acta Seismologica Sinica **2**, 447 (1980).
[13] H. K. P. Neubert, *Instrument Transducers* (Oxford University Press, Oxford, 1975).
[14] Mark Products, now Sercel Incorporated-USA, 17200 Park Row, Houston, Texas 77084-5935, http://www.sercel.com
[15] H. J. Paik, in *Proceedings of the Second Marcel Grossman Meeting on General Relativity*, edited by R. Ruffini (North–Holland, Amsterdam, 1982), p. 1193; also Phys. Rev. D **33**, 309 (1986).
[16] N. A. Haskel, Geophysics **14**, 558 (1949).
[17] W. H. Press, B. P. Flannery, S. A. Teukolsky, and W. T. Vetterling, *Numerical Recipes* (Cambridge University Press, Cambridge, 1986).